# Optical limiting property and mechanism of 2D MXene Nb<sub>2</sub>CT<sub>x</sub> nanosheets

# Lihe Yano,\* Yaoyao Ma, Jinhai Si, and Xun Hou

Xi'an Jiaotong University, Key Laboratory for Physical Electronics and Devices of the Ministry of Education and Shaanxi Key Laboratory of Photonic Technique for Information, School of Electronics Science and Engineering, Faculty of Electronic and Information Engineering, Xi'an, China

**Abstract.** We study the optical limiting (OL) property of a newly emerged MXene material, niobium carbide (Nb<sub>2</sub>CT<sub>x</sub>) nanosheets, using nanosecond laser Z-scan measurement. The nanosheets exhibited excellent OL property, and the OL thresholds are estimated to be about 0.35 and 0.44 J/cm<sup>2</sup> for 532 and 1064 nm, respectively. Compared with the traditional OL material, reduced graphene oxide, Nb<sub>2</sub>CT<sub>x</sub> nanosheets show a better OL property. The nonlinear scattering (NLS) measurements indicate that the excellent OL behavior of the nanosheets originates mainly from the strong NLS effect due to the good photothermal property of the material. © 2022 Society of Photo-Optical Instrumentation Engineers (SPIE) [DOI: 10.1117/1.OE.61.2.026108]

**Keywords:** optical limiting; MXene; nonlinear scattering.

Paper 20211141 received Oct. 7, 2021; accepted for publication Feb. 8, 2022; published online Feb. 23, 2022.

#### 1 Introduction

Optical limiting (OL) effect plays an important role in nonlinear optics areas, which is used for protecting optical sensors and human eyes from laser damage.  $^{1-3}$  An ideal optical limiter is required to be of low OL threshold and high-damage threshold and to be able to work in a wide spectral range.  $^{4,5}$  In the past decades, many efforts have been devoted in the developing of efficient OL materials, such as carbon-based nanomaterials including graphite, fullerenes, and carbon nanotubes (CNTs). Nevertheless, these materials could not meet the requirements mentioned above. For example,  $C_{60}$  shows strong reversed saturable absorption and strong OL property for 532-nm light, but it can only work in a very narrow spectral range. Some other materials such as carbon black suspension  $^{6-8}$  and CNTs  $^{9,10}$  can attenuate the strong laser in the broadband wavelength range through the nonlinear scattering (NLS) effect, but their limiting thresholds are too high to be applied in practice.

In recent years, two-dimensional (2D) graphene materials have attracted many researchers' attention due to their excellent optical and nonlinear optical properties. Chen et al. <sup>11</sup> first studied the OL properties of various graphene nanostructures, including graphene oxide nanosheets and nanoribbons, and graphene nanosheets and nanoribbons using a nanosecond laser at 532 and 1064 nm. Since then, many works have been reported about the nonlinear OL properties of graphene derivatives and some other 2D materials. <sup>12</sup> As a newly emerged 2D material, MXene nanosheets have caught researchers' attention in these few years. Generally, MXene nanosheets are prepared from ternary carbides and nitrides with MAX phases by etching the A element from  $M_{n+1}AX_n$ , where n=1,2, or 3, M is an early transition metal, A is an A-group (mostly groups 13 and 14) element, and X is C and/or N.<sup>13–15</sup> MXene has found applications in electrochemical capacitor, <sup>16</sup> electromagnetic interference shielding, <sup>17</sup> chemical catalyst, <sup>18</sup> and photothermal therapy. <sup>19</sup> Due to the narrow bandgap characteristics of the material,  $Ti_3C_2T_x$  (T=0, OH, or F, and the value of X is dependent on the degree of surface functionalization) nanosheets have shown excellent nonlinear optical response, such as nonlinear saturable absorption<sup>20</sup> and

0091-3286/2022/\$28.00 © 2022 SPIE

<sup>\*</sup>Address all correspondence to Lihe Yan, liheyan@mail.xitu.edu.cn

nonlinear refraction effect,<sup>21</sup> has been studied. However, the OL behavior of the material has been rarely reported.

Niobium carbide ( $Nb_2CT_x$ ) nanosheets are a newly emerged MXene material in recent years. Recently, Lin et al.<sup>22</sup> found that  $Nb_2CT_x$  nanosheets showed excellent near-infrared photothermal performance, and the photothermal conversion efficiency was estimated to be about 36.4% at NIR-I biowindow (750 to 1000 nm) and 45.65% at NIR-II biowindow (1000 to 1350 nm). This finding inspired our interest in investigating the OL property of the material for nanosecond pulsed laser. In the OL response in the nanosecond regime, the NLS effect, originating from the thermally induced solvent bubbles and microplasmas, plays an important role. <sup>11,12</sup> The good photothermal effect of the nanosheets could favor the conversion of the laser light to the heat absorbed by the material and the formation of scattering centers. Thereby, the  $Nb_2CT_x$  nanosheets with narrow bandgap and high photothermal conversion efficiency could exhibit excellent OL behavior for nanosecond laser pulses.

In this paper, we studied the nonlinear optical response of  $\mathrm{Nb_2CT_X}$  nanosheets dispersed in deionized water using nanosecond laser open aperture Z-scan method. The nanosheets showed a better OL property, compared with the reference sample of reduced graphene oxide (rGO). To clarify the nonlinear response mechanism of the material, NLS measurements were performed. The results indicated that the excellent OL behavior of the  $\mathrm{Nb_2CT_X}$  nanosheets could be attributed to the NLS effect, benefiting from the narrow bandgap and good photothermal performance of the material.

#### 2 Experimental Section

Nb<sub>2</sub>CT<sub>x</sub> nanosheets used in this work were purchased from Nanjing XFNano Materials Tech Co., Ltd., (Nanjing, China). The nanosheets with a thickness of 50 to 150 nm and an average diameter of about 1  $\mu$ m are multilayered. In our experiments, 30-mg multilayer Nb<sub>2</sub>CT<sub>x</sub> nanosheets were dispersed in 30 mL deionized water, and the mixture was ultrasonic processed in ice bath for 2 h to obtain uniform and stable dispersion. As the surface of Nb<sub>2</sub>CT<sub>x</sub> is rich in hydroxyl, oxygen, or fluorine and other functional groups, they showed good dispersibility in water. The prepared dispersion was filled in a 1-mm-thick quartz cell for nanosecond laser Z-scan measurement. As a comparison, rGO dispersion in water was prepared and used as the reference sample. By changing the solvent ratio, the linear transmittance of both Nb<sub>2</sub>CT<sub>x</sub> nanosheets and rGO dispersions were adjusted to be about 65%.

The morphology of  $Nb_2CT_x$  nanosheets was characterized using transmission electron microscope (TEM). The crystal structure of nanocrystalline tablets was analyzed with Shimazu x-ray diffractometer (XRD-7000). Raman spectra were obtained using a laser Raman spectrometer with excitation wavelength at 633 nm.

The OL characteristics of the materials were studied by nanosecond laser Z-scan technology. Figure 1 shows the experimental setup of the Z-scan measurements. A nanosecond Nd:YAG laser (10-ns pulses width, 1064-nm central wavelength, and 10-Hz repetition rate) was used in our experiment. After frequency doubling, 532-nm laser pulses can be obtained. The output laser pulses were focused by a lens (L1) with a focal length of 20 cm and the radius of the laser

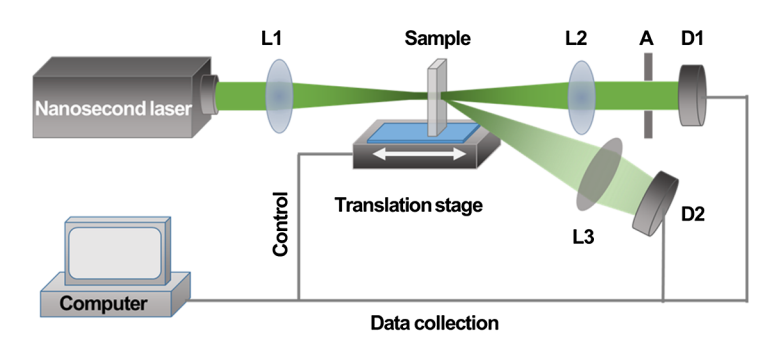


**Fig. 1** Schematic diagram of nanosecond *Z*-scan measurements. L1, L2, L3: lens; A: aperture; and D1, D2: detector.

beam at the focal point was estimated to be about 90  $\mu$ m. The transmitted light passing through the sample was collimated using another lens (L2), and transmitted pulse energy was monitored by an energy meter (D1). The sample was fixed on a translation stage, and by changing the distance between the sample and the laser focus, the nonlinear transmittance of the samples can be obtained as a function of Z position. To prevent the scattered light from entering D1, an aperture (A) was placed before the detector. The size of the aperture was slightly larger than the spot size, allowing all the transmitted light to pass through. To measure the NLS signals in the OL process, a part of the scattered light was collected by a lens (L3) into energy meter (D2) placed at an angle of 30 deg to the laser propagation direction.

## 3 Experimental Results and Discussions

First, the morphology of Nb<sub>2</sub>CT<sub>x</sub> nanosheet was observed using TEM. As shown in Fig. 2(a), the Nb<sub>2</sub>CT<sub>x</sub> nanosheet mainly exhibited as multilayers, presenting a typical 2D structure. The high-resolved TEM (HRTEM) images of nanosheets given by the inset of Fig. 2(a) show the highly crystalline nature with a lattice distance of 0.27 nm, being consistent with the (101) plane of the Nb<sub>2</sub>CT<sub>x</sub>. The absorption spectrum of Nb<sub>2</sub>CT<sub>x</sub> nanosheet is given in Fig. 2(b), which shows a broadband absorption in the visible-near-infrared region. Figure 2(c) presents the XRD patterns of the nanosheets. The newly emerged low-angle (002) peak is typical for most reported MXenes in Fig. 2(d), which implies that the sample has completely converted to MXenes (Nb<sub>2</sub>C). Algorithm 23,24 In addition, the XRD pattern of Nb<sub>2</sub>C reveals the disappearance of the most intense peaks of Nb<sub>2</sub>AlC at  $2\theta = 39$  deg because of the exfoliation of Al layer by HF. In Fig. 2(d), the Raman spectrum shows the *D* peak around 1330 cm<sup>-1</sup> and *G* peak around 1600 cm<sup>-1</sup> of carbon species which could be attributed to the breathing modes of rings and relative motion of sp<sup>2</sup>

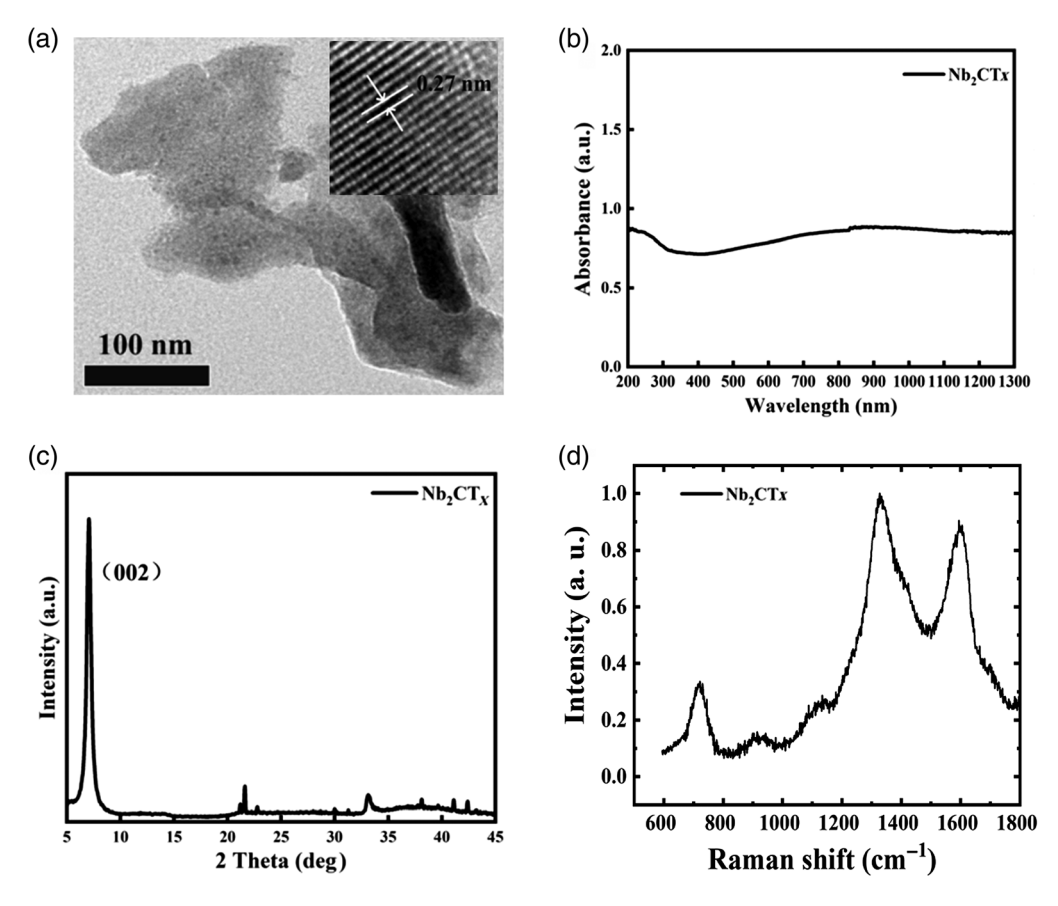


Fig. 2 (a) TEM and (b) HRTEM images, (c) UV-vis absorption spectrum, and (d) XRD patterns of the  $Nb_2CT_x$  nanosheets.

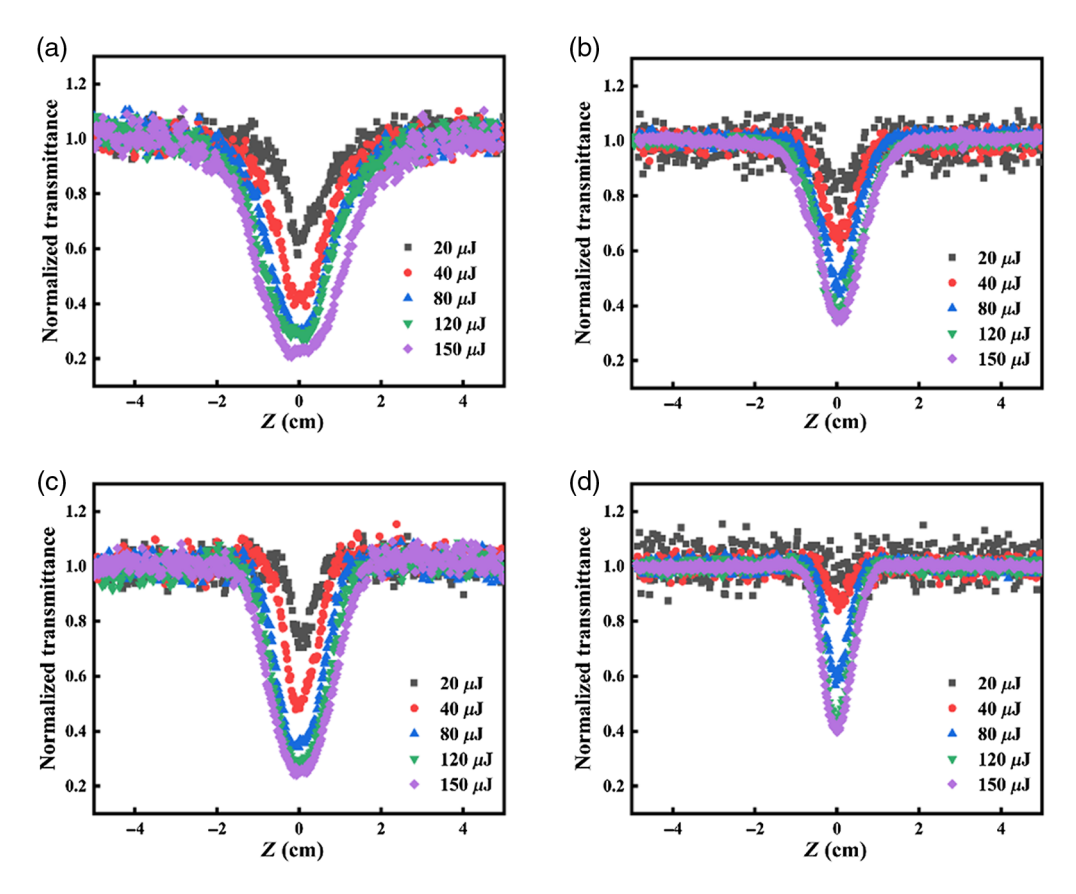


Fig. 3 The Z-scan curves of Nb<sub>2</sub>CT<sub>x</sub> nanosheets at (a) 532 nm and (b) 1064 nm and the reference sample of rGO at (c) 532 nm and (d) 1064 nm.

carbon atoms, respectively. An obvious peak at around 700 cm<sup>-1</sup> is also observed, which could be attributed the indication of Nb-C vibration.<sup>25</sup>

The nonlinear OL behavior of the Nb<sub>2</sub>CT<sub>x</sub> nanosheets for 532 and 1064 nm is studied using nanosecond laser Z-scan technique. Figures 3(a) and 3(b) show the OL properties of Nb<sub>2</sub>CT<sub>x</sub> dispersions at 532 and 1064 nm when the incident pulse energy changing from 20 to 150  $\mu$ J, respectively. From these figures, we can see that the transmittance of the material decreases obviously when the sample moves adjacent to the laser focus. With increasing the incident pulse energy, the nonlinear transmittance decreases rapidly. The results indicate that the Nb<sub>2</sub>CT<sub>x</sub> nanosheets exhibit strong nonlinear OL behavior for both 532 and 1064 nm laser pulses. In some previous reports, the nonlinear optical effect, especially saturable absorption effect has been observed in Nb<sub>2</sub>CT<sub>x</sub> nanosheets using ultrashort laser pulses. <sup>25,26</sup> The SA effect in the 2D material could be attributed to the optical bleaching of valence band and filling effect of conductive band under intense laser irradiation. As the recovery time of the excited electrons in the material ranged from 100 fs to ~ps, <sup>26</sup> much shorter than the duration of nanosecond laser pulses, the SA effect could be very weak in our nanosecond laser Z-scan measurements. Although SA effect has been also observed in nanosecond regime, the lower linear transmittance and shorter laser pulse duration could be responsible. <sup>27</sup>

As a reference, Z-scan measurements of rGO dispersion are performed under the same condition, the OL behavior of which has been deeply studied before. <sup>12</sup> The Z-scan results of rGO dispersion for 532 and 1064 nm laser are given in Figs. 3(c) and 3(d), respectively. Compared with the reference sample of rGO, the Z-scan curve of the sample decreases faster when the material moves to the focus than the reference sample under the same incident pulse energy. The results indicate that  $Nb_2CT_x$  nanosheets show stronger OL behavior than rGO dispersion.

Here we plot the normalized nonlinear transmittance as functions of the incident pulse energy density, both of rGO and  $Nb_2CT_x$  nanosheets dispersions. As shown by Figs. 4(a) and 4(b), the transmittance of both samples decrease with increasing the incident pulse energy density. The

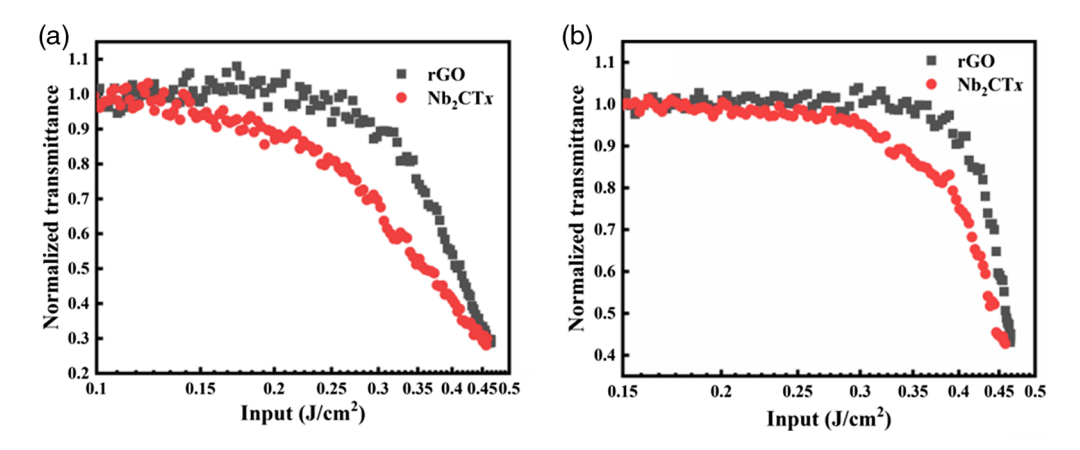


**Fig. 4**  $Nb_2CT_x$  and RGO normalized transmittance in dependence on the incident pulse energy density at (a) 532 nm and (b) 1064 nm.

OL threshold of  $Nb_2CT_x$  nanosheets, defined as the pulse energy density when the nonlinear transmittance falls to 50% of the linear transmittance, were measured to be 0.35 J/cm<sup>2</sup> at 532 nm and 0.44 J/cm<sup>2</sup> at 1064 nm. These OL thresholds were lower than those in the referenced rGO dispersion, which were estimated to be about 0.42 J/cm<sup>2</sup> at 532 nm and 0.46 J/cm<sup>2</sup> at 1064 nm, respectively. The OL property of  $Nb_2CT_x$  was also compared with other 2D materials, such as layered transition metal dichalcogenide nanosheets<sup>4</sup> and black phosphorus materials, and the OL thresholds of  $Nb_2CT_x$  were several times lower.<sup>28</sup>

In the OL process of materials, different nonlinear optical effects including NLS, nonlinear absorption, and nonlinear refraction might contribute. In our experiments, the transmitted laser beam was collimated by a lens, and the spot size incident into the detector was much smaller than the aperture of detector. Hence, nonlinear refraction effect could be ruled out. To clarify the OL mechanism of the sample, we measured the NLS signal intensity in Z-scan measurements. Figure 5(a) gives the transmitted and scattered light intensity change when the sample moves along the Z direction. From this figure, we can see that the onset of the growth/decrease of scattered signals is synchronous with the onset of the decrease/growth of transmission. Figure 5(b) shows the transmitted and scattered light intensity change by varying the incident pulse energy density. The results indicate that the NLS effect is mainly responsible for the OL property of the Nb<sub>2</sub>CT<sub>x</sub> nanosheets dispersion.

According to the theoretical analysis of the NLS effect in nanomaterial suspensions (such as CNTs and graphene materials), when laser light incidents into the dispersion, nanomaterials could absorb the light energy and be heated. The surrounding solvents would be evaporated due to the heat transfer from the nanomaterial, resulting in the formation of gas bubbles, and which would expand rapidly because of the high temperature and pressure. When the size of the

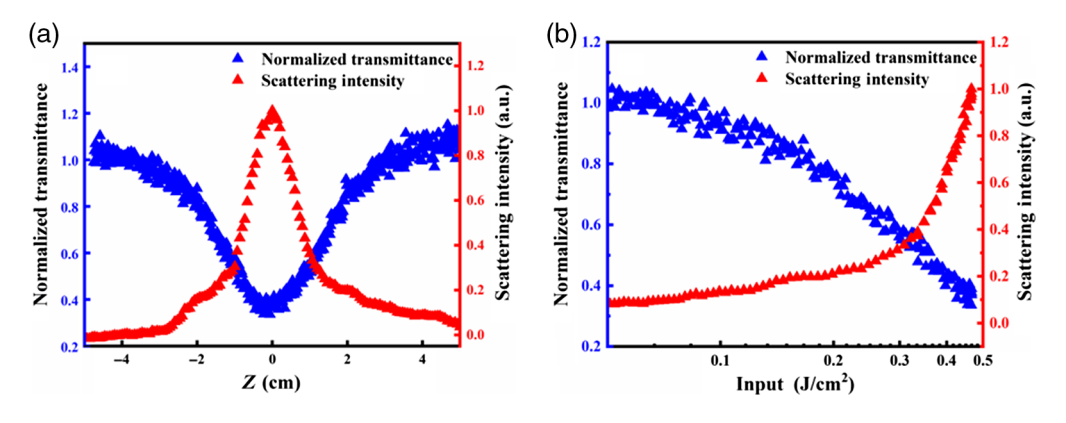


Fig. 5 The transmitted and scattered light intensity change in dependence on (a) Z position and (b) pulse energy density of the incident laser.

bubbles is comparable to the incident light wavelength, NLS effect could take place, effectively limiting the incident laser power. In this process, two factors could influence the NLS intensity seriously: the absorption of the incident light by the material, and the photothermal conversion efficiency revealing the ability of the material in converting light into heat. The optical absorption spectra of Nb<sub>2</sub>CT<sub>x</sub> nanosheets show a broad and strong absorption band covering the visible- and near-infrared region. The photothermal conversion efficiency of the material has been demonstrated to be significantly higher than those of some representative photothermal agents in phototherapy, such as gold nanorods and graphene.<sup>22</sup> These two features of Nb<sub>2</sub>CT<sub>x</sub> nanosheets make the NLS effect occur easily in dispersion. As the reference, the OL mechanism in rGO dispersions in water has been demonstrated to be attributed to the NLS effect.<sup>12,29</sup> Although the graphene material also has broadband absorption in the visible- to near-infrared wavelength regions, the higher photothermal conversion efficiency caused the better OL property of the Nb<sub>2</sub>CT<sub>x</sub> nanosheets.

#### 4 Conclusion

In summary, we study the nonlinear OL properties of 2D MXene material, niobium carbide  $(Nb_2CT_x)$  nanosheets, using nanosecond laser Z-scan methods. The  $Nb_2CT_x$  nanosheets dispersion shows excellent OL properties both at 532 and 1064 nm, the OL thresholds of which are established to be about 0.35 and 0.44  $J/cm^2$ , respectively. By measuring the NLS signals as a function of the incident pulse energy density, we found that the NLS effect is mainly responsible for the OL behavior of the material. The unique features of the  $Nb_2CT_x$  nanosheets, strong absorption and high photothermal conversion efficiency in the visible- to near-infrared region, make the NLS effect take place easily in dispersion and be of benefit to the OL property of the material. Nevertheless, the OL thresholds are still much higher than the maximum permissible exposure for ocular exposure, and the combination of OL devices and traditional laser protective glasses may be more practical.

## Acknowledgments

This work was supported by the National R&D Program of China (No. 2019YFA0706402), the National Natural Science Foundation of China (Nos. 62027822 and 61690221), and the Key Research and Development Program of Shaanxi Province (No. 2017ZDXM-GY-120). The authors declare no conflicts of interest.

## References

- 1. L. Vivien et al., "Pulse duration and wavelength effects on the optical limiting behavior of carbon nanotube suspensions," *Opt. Lett.* **26**(4), 223–225 (2001).
- 2. L. Vivien et al., "Carbon nanotubes for optical limiting," Carbon 40(10), 1789–1797 (2002).
- 3. K. C. Chin et al., "Modified carbon nanotubes as broadband optical limiting nanomaterials," *J. Mater. Res.* **21**(11), 2758–2766 (2006).
- 4. N. Dong et al., "Optical limiting and theoretical modelling of layered transition metal dichalcogenide nanosheets," *Sci. Rep.* **5**, 14646 (2015).
- 5. Y. Zhang et al., "Poly(arylene ether)s with aromatic azo-coupled cobalt phthalocyanines in the side chain: synthesis, characterization and nonlinear optical and optical limiting properties," *RSC Adv.* **9**(16), 9253–9259 (2019).
- 6. R. C. Hollins, "Materials for optical limiters," *Curr. Opin. Solid State Mater. Sci.* **4**(2), 189–196 (1999).
- 7. K. Mansour, M. J. Soileau, and E. W. Van Stryland, "Nonlinear optical properties of carbon-black suspensions (ink)," *J. Opt. Soc. Am. B* **9**(7), 1100–1109 (1992).
- 8. K. M. Nashold and D. P. Walter, "Investigations of optical limiting mechanisms in carbon particle suspensions and fullerene solutions," *J. Opt. Soc. Am. B* **12**(7), 1228–1237 (1995).

- 9. P. Chen et al., "Electronic structure and optical limiting behavior of carbon nanotubes," *Phys. Rev. Lett.* **82**(12), 2548–2551 (1999).
- N. Kamaraju et al., "Large nonlinear absorption and refraction coefficients of carbon nanotubes estimated from femtosecond z-scan measurements," *Appl. Phys. Lett.* 91(25), 251103 (2007).
- 11. M. Feng, H. Zhan, and Y. Chen, "Nonlinear optical and optical limiting properties of graphene families," *Appl. Phys. Lett.* **96**(3), 033107 (2010).
- 12. Y. Chen et al., "Graphene and its derivatives for laser protection," *Prog. Mater. Sci.* **84**, 118–157 (2016).
- 13. M. Naguib et al., "Two-dimensional nanocrystals produced by exfoliation of Ti<sub>3</sub>AlC<sub>2</sub>," *Adv. Mater.* **23**(37), 4207–4207 (2011).
- 14. P. Eklund et al., "The  $M_{n+1}AX_n$  phases: materials science and thin-film processing," *Thin Solid Films* **518**(8), 1851–1878 (2010).
- 15. M. Naguib et al., "Two-dimensional transition metal carbides," *ACS Nano* **6**(2), 1322 (2012).
- 16. M. Zhu et al., "Highly flexible, freestanding supercapacitor electrode with enhanced performance obtained by hybridizing polypyrrole chains with Mxene," *Adv. Energy Mater.* **6**(21), 1600969 (2016).
- 17. F. Shahzad et al., "Electromagnetic interference shielding with 2D transition metal carbides (MXenes)," *Science* **353**(6304), 1137–1140 (2016).
- 18. X. Xie et al., "Surface Al leached Ti<sub>3</sub>AlC<sub>2</sub> as a substitute for carbon for use as a catalyst support in a harsh corrosive electrochemical system," *Nanoscale* **6**(19), 11035–11040 (2014).
- 19. J. Xuan et al., "Organic-base driven intercalation and delamination for the production of functionalized titanium carbide nanosheets with superior photothermal therapeutic performance," *Angew. Chem.* **128**(47), 14789–14794 (2016).
- 20. L. Wu et al., "MXene-based nonlinear optical information converter for all-optical modulator and switcher," *Laser Photonics Rev.* **12**(12), 1800215 (2018).
- 21. J. Li et al., "Broadband spatial self-phase modulation and ultrafast response of MXene  $Ti_3C_2T_x$  (T = O, OH or F)," *Nanophotonics* **9**(8), 2415–2424 (2020).
- 22. H. Lin et al., "A two-dimensional biodegradable niobium carbide (MXene) for photothermal tumor eradication in NIR-I and NIR-II biowindows," *J. Am. Chem. Soc.* **139**(45), 16235 (2017).
- 23. P. Urbankowski et al., "Synthesis of two-dimensional titanium nitride Ti<sub>4</sub>N<sub>3</sub>(MXene)," *Nanoscale* **8**(22), 11385–11391 (2016).
- 24. J. Zhou et al., "A two-dimensional zirconium carbide by selective etching of Al<sub>3</sub>C<sub>3</sub> from nanolaminated Zr<sub>3</sub>Al<sub>3</sub>C<sub>5</sub>," *Angew. Chem. Int. Ed.* **55**(16), 5008–5013 (2016).
- 25. Z. Niu et al., "Theoretical and experimental investigations on Nb<sub>2</sub>CT<sub>x</sub> MXene Q-switched Tm:YAP laser at 2 μm for the nonlinear optical response," *Nanotechnology* **32**, 375709 (2021).
- 26. Y. Wang et al., "Niobium carbide MXenes with broad-band nonlinear optical response and ultrafast carrier dynamics," *ACS Nano* **14**(8), 10492–10502 (2020).
- 27. C. Chen et al., "Switchable nonlinear absorption and ultrafast dynamics process of Nb<sub>2</sub>CT<sub>x</sub>," *Ferroelectrics* **581**(1), 40–46 (2021).
- 28. M. Shi et al., "Donor–acceptor type blends composed of black phosphorus and C<sub>60</sub> for solid-state optical limiters," *Chem. Commun.* **54**(4), 366–369 (2018).
- 29. L. Yan et al., "Optical limiting properties and mechanisms of single-layer graphene dispersions in heavy-atom solvents," *Opt. Express* **22**(26), 31836–31841 (2014).

Biographies of the authors are not available.